

258493



NHTSA - 98-3585-55

**General Motors Corporation
Legal Staff**

Facsimile
(586) 492-2928

Telephone
(586) 947-9212

DEC 20 2002

Annette M. Sandberg,
Deputy Administrator
NATIONAL HIGHWAY TRAFFIC
SAFETY ADMINISTRATION
400 Seventh Street, S.W., Room 5220
Washington, DC 20590

Dear Ms. Sandberg:

Re: **Settlement Agreement**
Section B. Fire Safety Research

Enclosed is a paper prepared by Jeffrey Santrock of General Motors Corporation and Archibald Tewarson and Peter K. S. Wu of Factory Mutual Research Corporation, entitled, "Flammability Testing of Automotive Heating Ventilation and Air Conditioning Modules Made From Polymers Containing Flame Retardant Chemicals." It relates to Project B.10 (Study of Flammability of Materials).

This paper was presented at and included in the proceedings of the 2002 SAE International Truck and Bus Meeting and Exhibition held in Detroit, Michigan, November 18-20, 2002. NHTSA was advised in advance of this presentation.

Yours truly,

Deborah K. Nowak-Vanderhoef
Attorney

Enclosure

**Flammability Testing of Automotive Heating
Ventilation and Air Conditioning Modules
Made from Polymers Containing
Flame Retardant Chemicals**

Jeffrey Santrock
General Motors Corporation

Archibald Tewarson and Peter K. S. Wu
Factory Mutual Research Corporation

All rights reserved. No part of this publication may be reproduced, stored in a retrieval system, or transmitted, in any form or by any means, electronic, mechanical, photocopying, recording, or otherwise, without the prior written permission of SAE.

For permission and licensing requests contact:

SAE Permissions
400 Commonwealth Drive
Warrendale, PA 15096-0001-USA
Email: permissions@sae.org
Fax: 724-772-4891
Tel: 724-772-4028



For multiple print copies contact:

SAE Customer Service
Tel: 877-606-7323 (inside USA and Canada)
Tel: 724-776-4970 (outside USA)
Fax: 724-776-1615
Email: CustomerService@sae.org

ISBN 0-7680-1109-4
Copyright © 2002 SAE International

Positions and opinions advanced in this paper are those of the author(s) and not necessarily those of SAE. The author is solely responsible for the content of the paper. A process is available by which discussions will be printed with the paper if it is published in SAE Transactions.

Persons wishing to submit papers to be considered for presentation or publication by SAE should send the manuscript or a 300 word abstract of a proposed manuscript to: Secretary, Engineering Meetings Board, SAE.

Printed in USA

Flammability Testing of Automotive Heating Ventilation and Air Conditioning Modules Made from Polymers Containing Flame Retardant Chemicals

Jeffrey Santrock
General Motors Corporation

Archibald Tewarson and Peter K. S. Wu
Factory Mutual Research Corporation

Copyright © 2002 SAE International

ABSTRACT

Flammability tests were conducted on one control HVAC module and two experimental automotive HVAC modules containing flame retardant chemicals. The HVAC modules were exposed to a heptane pool fire. All three HVAC modules burned under these conditions. The mass loss rates of the control and experimental HVAC modules were similar. The flame retardant chemicals caused a 50% reduction in the heat produced, a 751 – 897% increase in the carbon monoxide produced, a 4,867 – 5,567% increase in the gaseous hydrocarbon produced, and a 3,875 – 4,725% increase in the smoke produced when the HVAC modules burned under these conditions. These quantitative results are consistent with visual observations made during these tests that the experimental HVAC modules produced substantially more smoke than the control HVAC module.

INTRODUCTION

Chemical flame retardants are used to modify the flammability properties of polymeric materials. One effect of adding a chemical flame retardant to a polymer may be greater resistance to ignition of a polymer containing flame retardant compared to the same polymer without flame retardant. Once ignition occurs, the presence of a flame retardant in a polymer may result in a slower rate of flame spread compared to the same polymer without flame retardant. Some flame retardants alter both resistance to ignition and rate of flame spread, while other flame retardants alter only one of these parameters.

Flame retardant additives act by interfering with one or more of the basic steps in the combustion of polymeric materials [1 – 5]. These steps have been described as

have been described as heat transfer to the polymer, thermal decomposition of the polymer, mass transfer of volatile fuels produced by thermal decomposition to the gas phase, and chemical reactions of the volatile fuels with oxygen (oxidation) to produce heat and combustion by-products [1 – 5].

- Reduce Heat Transfer to the Polymer. One approach to reducing heat transfer to the polymer is to add flame retardants that promote the formation of a carbonaceous char or a glassy film on the surface of a polymer during combustion. These surface coatings can act as thermal insulations that reduce heat transfer from the flame into the polymer, which results in lower temperatures in the polymer and lower rates of thermal decomposition of the polymer.
- Reduce the Thermal Decomposition Rate of Polymer. Compounds that undergo endothermic dehydration when heated can reduce the temperature of the polymer, thus reducing the rates of thermal decomposition of the polymer and production of volatile fuels from the polymer. The water vapor formed in this process can also reduce the concentration of O₂ at the surface of the polymer, which can interfere with flame chemistry (see below).
- Reduce the Mass Transfer Rate of Volatile Fuels to the Gas Phase. Carbonaceous char and glassy films also can act as physical barriers that inhibit the release of gaseous fuel from the decomposed polymer. This results in lower rates of fuel volatilization into the combustion zone.

- Interfere with Flame Chemistry. Inert gases or active chemical species produced by thermal decomposition of the polymer or chemical additives to the polymer can interfere with exothermic chemical reactions in the combustion zone. Active chemical species such as certain halogen-, antimony-, or phosphorous-containing gases terminate the exothermic free radical chain reactions involving hydrogen ($H\bullet$) and hydroxyl ($HO\bullet$) radicals in the flame. Inert gases displace air at the surface of the polymer, reducing the amount of oxygen available for reaction in the flame. Inert gases produced by thermal decomposition of chemical additives to the polymer can displace the amount of O_2 available for reaction with the volatile fuels by displacing air from the combustion zone. Inert gases also appear to reduce the temperature in the combustion zone, slowing the rate of oxidation of volatile fuels.

A large number of phosphorous-containing flame retardant additives act by increasing the amount of carbonaceous char formed on the surface of the polymer when it burns. The chemical mechanism of char promotion by phosphorous-containing flame retardants is thought to involve dehydration of the polymer by formation of phosphoric acid during combustion. [6 - 8]. Triphenylphosphene oxide appears to produce one or more gaseous thermal decomposition products that actively interfere with flame chemistry [9].

In addition to promotion of surface charring, aluminum silicate ($Al_2O_3 \cdot (SiO_2)_x$) is thought to act by formation of a glassy layer on the surface of the polymer during combustion.

Flame retardants that contain fluorine, chlorine, bromine, or iodine (halogens) act by producing gases that terminate the free-radical chain reactions occurring in the flame. Thermal decomposition of the flame retardant yields hydrogen halide gas. The hydrogen halide reacts with hydrogen ($H\bullet$) and hydroxyl ($HO\bullet$) radicals in the flame forming H_2 and H_2O , respectively [10, 11]. The hydrogen halide is regenerated during these chemical reactions, so it acts as a catalytic free-radical scavenger resulting in termination of the free radical chain reactions in the flame. Halogen can be incorporated into a polymer as part of the molecular structure of the polymer itself or by mixing a halogen-containing blending into the polymer. An example of a polymer that contains halogen as part of the molecular structure of the polymer is poly(vinyl chloride), which produces hydrogen chloride (HCl) upon thermal decomposition and is inherently flame retardant [13]. One of the more widely used chemical halogen-containing flame retardant additives is decabromodiphenylene oxide (DBDO), which forms hydrogen bromide (HBr) on thermal decomposition.

Antimony compounds such as antimony trioxide (Sb_2O_3) are often used in combination with halogen-based to enhance flame retardant effects. The active species here is antimony trichloride ($SbCl_3$) [12 - 15]. In addition to being a free radical scavenger, it has been suggested that $SbCl_3$, which is denser and more viscous than air, also reduces the concentration of O_2 at the surface of the polymer [2].

Compounds such as aluminum hydroxide ($Al(OH)_3$), hydrated alumina ($Al_2O_3 \cdot 3H_2O$), and magnesium hydroxide ($Mg(OH)_2$) undergo endothermic dehydration when heated, cool the polymer during combustion and thus reducing the rate of polymer decomposition and production of volatiles [16]. The water vapor formed is also thought to reduce the concentration of O_2 at the surface of the polymer [2].

Regardless of the chemical mechanism, the net effect of flame retardant additives is to reduce the heat release rate during combustion. Depending on the concentration of flame retardant in the polymer, the thermal decomposition temperature of the flame retardant relative to that of the polymer, and other factors, a lower heat release rate in the combustion zone can result in a greater resistance to ignition, slower flame spread rates during the early stages of the fire, or both. Flame retardants become less effective or ineffective in inhibiting ignition as the energy of the ignition source increases [1 - 2]. The effect of flame retardants in slowing flame spread is diminished once the fire becomes established [1 - 2]. One potential consequence of delaying ignition and reducing the efficiency of combustion once ignition has occurred is increasing the production of incomplete combustion products such as carbon monoxide, hydrogen cyanide, particulate (smoke), and other pyrolysis products [17].

This report describes results of flammability tests conducted to determine the effect of chemical flame retardants on the flammability properties of automotive Heating Ventilation and Air Conditioning (HVAC) modules, including heat release, production of smoke, carbon dioxide, carbon monoxide, and unoxidized and partially oxidized organic compounds. One control and two experimental HVAC modules were used in these tests. The HVAC modules were assemblies containing poly(propylene), polyester, nylon, and metal components. The plastic materials in the control HVAC module did not contain flame retardant chemicals. The poly(propylene) materials in the experimental HVAC modules contained antimony trioxide, decabromodiphenylene oxide, and zinc-based flame retardants. Two different flame retardant formulations were used in the polyester materials in the experimental HVAC modules. The polyester materials in one of the experimental HVAC modules contained antimony trioxide and aluminum silicate. The polyester materials

in the other experimental HVAC module contained hydrated alumina.

The HVAC modules were exposed to flames from a heptane pool fire. The mass loss rate from the HVAC assemblies, oxygen consumption rate, and release rates of carbon dioxide, carbon monoxide, hydrocarbons (unoxidized and partially oxidized organic compounds) and smoke (particulate) from the fire were measured during these tests. The convective and chemical heat release rates of the heptane igniter and the three HVAC modules were determined from this data.

MATERIALS AND METHODS

HVAC MODULES - The HVAC modules used in this test were for a 1999 Chevrolet Camaro. Table 1 lists the materials and masses of selected components in this HVAC module assembly.

Table 1 - Material and Mass of HVAC Parts

Component	Material ¹	Mass (kg)
Air Inlet and Outlet Housing	PP	0.27
Auxiliary A/C Evaporator and Blower Upper Case	PP	0.55
Auxiliary A/C Evaporator and Blower Lower Case	PE	2.03
Heater Front Case	PP	0.58
Heater Rear Case	PP	0.31
Heater Case	PP	0.24
Air Distribution Case	PP	0.58
A/C Evaporator Core	AL	1.86
Heater Core	AL	0.64
Mode Valve	ST	0.26
Blower Motor	M	1.31
HVAC Module	n/a	9.70

¹ AL = Aluminum, M = metal; PE = polyester; PP = poly(propylene), ST = Steel.

None of the materials in the control HVAC module used in these tests contained flame retardant chemicals. The poly(propylene) and polyester parts in the two experimental HVAC modules used in these tests contained flame retardant chemicals.

Table 2 lists chemical additives in the poly(propylene) and polyester components in the HVAC assembly. The Air Inlet and Outlet Housing, Auxiliary A/C Evaporator and Blower Upper Case, Heater Front Case, Heater Rear Case, Heater Case, and Air Distribution Case were molded from poly(propylene) resin containing decabromodiphenylene oxide (DBDO), antimony trioxide

(SbO₃), and zinc-based compounds (Table 2). Auxiliary A/C Evaporator and Blower Lower Cases were molded from polyester resins containing antimony trioxide and alumina silicate (Al₂O₃•(SiO₂)) or alumina hydrate (Al₂O₃•H₂O) chemicals (Table 2). The experimental HVAC modules were designated FR1 and FR2 to indicate the different flame retardant chemical formulations in the Auxiliary A/C Evaporator and Blower Lower Cases. The poly(propylene) components in FR1 and FR2 were the same.

Table 2 - Chemical Additives in the Poly(propylene) and Polyester Components¹

	poly(propylene)	polyester
Control	Ca(CO ₃)	glass fiber clay cissel
FR1	DBDO SbO ₃ Zn-compounds	glass fiber SbO ₃ Al ₂ O ₃ •(SiO ₂)
FR2	DBDO SbO ₃ Zn-compounds	glass fiber Al ₂ O ₃ •3H ₂ O

¹ Ca(CO₃) = calcium carbonate; DBDO = decabromodiphenylene oxide; SbO₃ = antimony trioxide; Al₂O₃•(SiO₂) = aluminum silicate; Al₂O₃•3H₂O = hydrated alumina.

FIRE PRODUCTS COLLECTOR

Heat and combustion gases generated by the burning HVAC modules were measured with a fire products collector [18] (Fig. 1).

The fire products collector consisted of a collection funnel (diameter = 6.1 m), an orifice plate (hole = 0.9 m), and a vertical stainless steel sampling duct (diameter = 1.5 m). The sampling duct was connected to the air pollution control system of the Test Center. The blower of the air pollution control system induces gas flow through the sampling duct. Air enters the sampling duct via the orifice plate. The temperature, linear velocity, optical transmission, and chemical composition of the entrained gas were measured in the center of the sampling duct 8.66 m (5.7 duct diameters) downstream from the orifice plate, ensuring a flat velocity profile at the sampling location. The data acquisition system consisted of a Hewlett Packard 2313B analog-to-digital conversion sub-system interfaced to a Hewlett Packard 1000 computer.

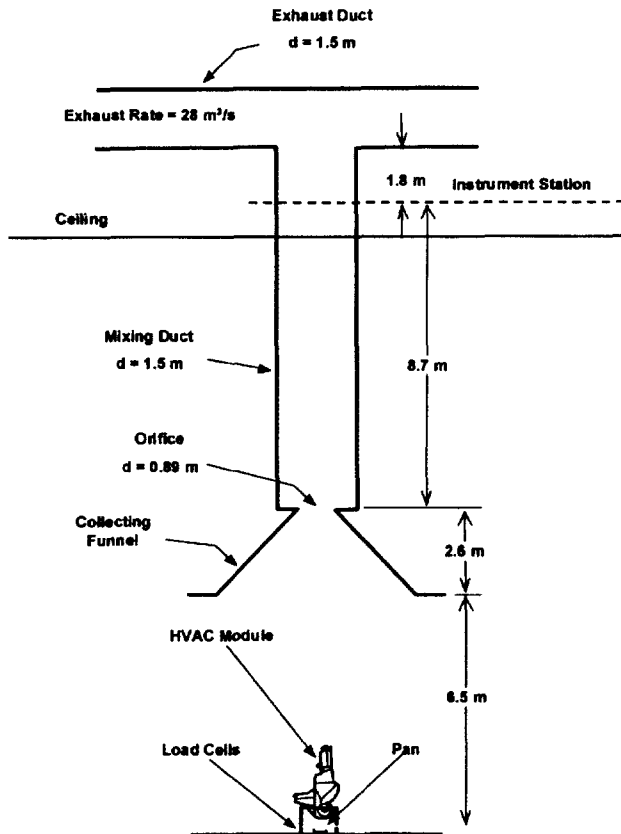


Figure 1. Diagram of an HVAC module under the fire products collector.

Gas temperature in the sampling duct was measured with two Type-K thermocouples (30 gage) with exposed bead-type junctions. The thermocouple leads were housed in stainless steel tubes (o.d. = 6.4 mm). Ambient air temperature in the facility was measured by five Type-K thermocouples attached to the external surface of the duct at 2.44, 5.49, 9.14, 12.8, and 15.9 m above the floor. These thermocouples were shielded from radiation from the fire.

The linear velocity of the gas entrained in the sampling duct was measured with a Pitot ring consisting of four Pitot tubes. A static pressure tap was mounted on the inside wall of the sampling duct. The pressure difference between the Pitot ring and the static wall tap was measured with an electronic manometer (Barocel Model 1173, CGS Scientific Corporation).

The particulate concentration in the entrained air was determined from the optical transmission across the duct measured at 0.4579 μm (blue), 0.6328 μm (red), and 1.06 μm (infrared). The optical path length across the duct was 1.524 m. Gas was withdrawn from the sampling duct through a stainless steel tube (o.d. = 3.9 mm) at a flow rate of $0.17 \times 10^{-3} \text{ m}^3/\text{s}$ for chemical analysis. The gas flowed through a particulate filter, a water condenser, and a drying agent before entering the

analyzers. Carbon dioxide (CO_2) and carbon monoxide (CO) were measured with two non-disperse infrared analyzers (Beckman Model 864 Infrared Analyzers). Oxygen (O_2) was measured with a paramagnetic oxygen analyzer (Beckman Model 755 Paramagnetic Oxygen Analyzer). The concentration of the mixture of gaseous hydrocarbons (total hydrocarbons) was measured with a flame ionization analyzer (Beckman Model 400 Flame Ionization Analyzer).

The rate of product release G_j was calculated using the following relationship:

$$G_j = \left(\frac{dR_j}{dt} \right) = f_j \left(\frac{dV}{dt} \right) \rho_j = f_j \left(\frac{dW}{dt} \right) \left(\frac{\rho_j}{\rho_g} \right) \quad (1)$$

where $d(R_j)/dt$ is the mass release rate of product j in kg/s ; f_j is the volume fraction of product j ; dV/dt is the total volume flow rate of the gas entrained in the sampling duct in m^3/s ; dW/dt is the total mass flow rate of the gas entrained in the sampling duct in kg/s ; ρ_j is the density of product j in g/m^3 ; and ρ_g is the density of the gas entrained in the concentration measurements in g/m^3 . The rate of oxygen consumption was calculated using equation (1), where the volume fraction of oxygen consumed was substituted for f_j .

The volume fraction of smoke particulate (f_s) was calculated from the following relationship:

$$f_s = \frac{D\lambda \times 10^{-6}}{\Omega} \quad (2)$$

where f_s is the volume fraction of smoke, λ is the wavelength of the light source, Ω is the extinction coefficient of particulate (a value of 7.0 was used in these calculations), and D is the optical density at each of the three wavelengths at which measurements were made:

$$D = \frac{\ln(I_0/I)}{L} \quad (3)$$

where I_0 is the intensity of light transmitted through clean air, I is the intensity of light transmitted through air containing smoke particulate, and L is the optical path length, which was equal to 1.524 m. A value of $1.1 \times 10^6 \text{ g/m}^3$ was used for the density of smoke particulate (ρ) in equation (1).

The convective heat release rate (Q_{conv}) was calculated using the following relationship:

$$Q_{\text{conv}} = \left(\frac{dE_{\text{conv}}}{dt} \right) = c_p (T_g - T_a) \left(\frac{dW}{dt} \right) \quad (4)$$

dW/dt is the mass flow rate of the gas entrained in the sampling duct in kg/s; c_p is the heat capacity of the gas entrained in the sampling duct at the gas temperature in kJ/(kg×K); T_g is the temperature of the gas entrained in the sampling duct in K; and T_a is the ambient air temperature in K.

The chemical heat release rate was calculated from the release rates of carbon dioxide and carbon monoxide ($Q_{CHEM}^{CO_2}$) as follows:

$$Q_{CHEM}^{CO_2} = \left(\frac{dE_{CHEM}}{dt} \right) = \Delta H_{CO_2}^* \left(\frac{dR_{CO_2}}{dt} \right) + \Delta H_{CO}^* \left(\frac{dR_{CO}}{dt} \right) \quad (5)$$

$\Delta H_{CO_2}^*$ is the net heat of complete combustion per unit mass of carbon dioxide released by the fire in kJ/g; ΔH_{CO}^* is the net heat of complete combustion per unit mass of carbon monoxide released by the fire in kJ/g; dR_{CO_2}/dt is the mass release rate of carbon dioxide in kg/s; and dR_{CO}/dt is the mass release rate of carbon monoxide in kg/s. Values of $\Delta H_{CO_2}^*$ and ΔH_{CO}^* were obtained from the literature [19].

The chemical heat release rate also was calculated from the oxygen consumption rate ($Q_{CHEM}^{O_2}$) as follows:

$$Q_{CHEM}^{O_2} = \left(\frac{dE_{CHEM}}{dt} \right) = \Delta H_{O_2}^* \left(\frac{dC_{O_2}}{dt} \right) \quad (6)$$

where $d(E_{CHEM})/dt$ is the chemical heat release rate in kW; $\Delta H_{O_2}^*$ is the net heat of complete combustion per unit mass of O_2 consumed in kJ/g; and $d(C_{O_2})/dt$ is the consumption rate of oxygen in kg/s. The value for $\Delta H_{O_2}^*$ was obtained from the literature [19].

Mass loss from the burning HVAC modules was measured with a load cell weigh-module system (KIS Series, BLH Electronics, Inc.) on a support stand.

Flammability Tests

Each HVAC module was mounted to a stand so that the module was oriented vertically. The base of the stand was 6.5 m below the opening of the collection duct of the Fire Products Collector. The ignition source for the HVAC modules was a pool of heptane (1450 mL) contained in a metal pan (9 in. x 9 in.) located below the center of the HVAC module. The heptane was ignited using a propane torch.

Results

Approximately 58% (wt/wt) of the HVAC modules used in these tests consisted of organic polymers (plastics), while metals comprised the remaining and 42% (wt/wt) (Table 1). The poly(propylene) and polyester parts

containing flame retardant chemical additives constituted approximately 81% (wt/wt) of the combustible materials in the two experimental HVAC modules (Table 1).

In these fire tests, the HVAC modules ignited between 30 and 60 seconds after ignition of the heptane. The heptane ignition source burned for approximately 11 minutes, and the HVAC modules were allowed to burn for an additional 4 to 5 minutes after the heptane was consumed.

Data recorded from the fire products collector included ambient air temperature, barometric pressure, gas temperature, gas flow rate, carbon dioxide concentration (C_{CO_2}), carbon monoxide concentration (C_{CO}), total hydrocarbons concentration (C_{HC}), oxygen concentration (C_{O_2}), turbidity at $\lambda = 0.4679 \mu\text{m}$, turbidity at $\lambda = 0.6318 \mu\text{m}$, and turbidity at $1.06 \mu\text{m}$. Data from the load cells on the HVAC module test stand also was recorded to determine mass loss from HVAC modules.

Mass loss curves for the control HVAC module, the FR1 HVAC module, the FR2 HVAC module, and the heptane ignition source are shown in Figure 2.

Plots of the carbon dioxide release rates (G_{CO_2}), carbon monoxide release rates (G_{CO}), hydrocarbon release rates (G_{HC}), and oxygen consumption rates (G_{O_2}) for the control + heptane ignition source, the FR1 HVAC module + heptane ignition source, the FR2 HVAC module + heptane ignition source, and the heptane ignition source are shown in Figures 3 through 6. G_{CO_2} , G_{CO} , G_{HC} , and C_{O_2} were determined from the C_{CO_2} , C_{CO} , C_{HC} , and C_{O_2} data using equation 1.

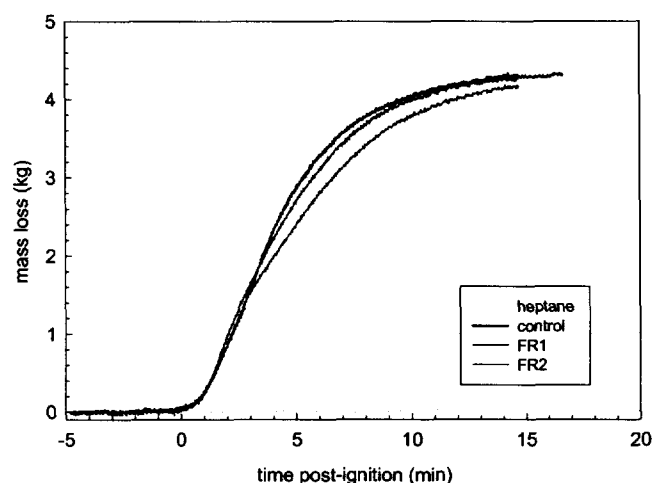


Figure 2. Mass loss curves.

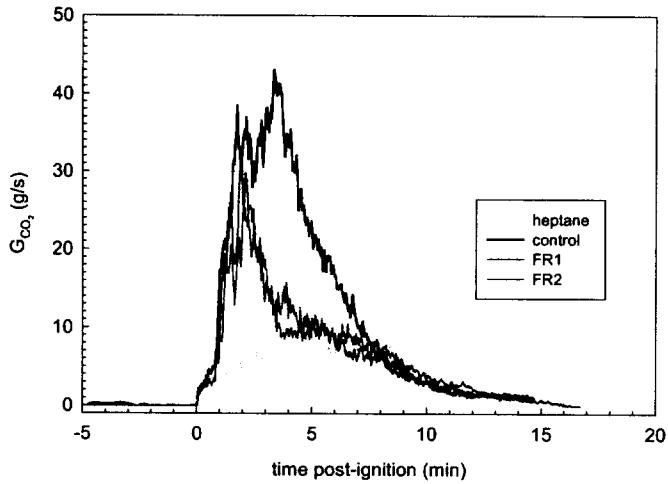


Figure 3. Carbon dioxide release rate (G_{CO_2}) curves.

Plots of the smoke release rate (G_{SMOKE}) for the control HVAC module, the two experimental HVAC modules, and the heptane ignition source are shown in Figure 7. C_{SMOKE} was determined from the turbidity at $\lambda = 0.6318 \mu m$ data using equations 2 and 3. G_{SMOKE} was determined from C_{SMOKE} using equation 1.

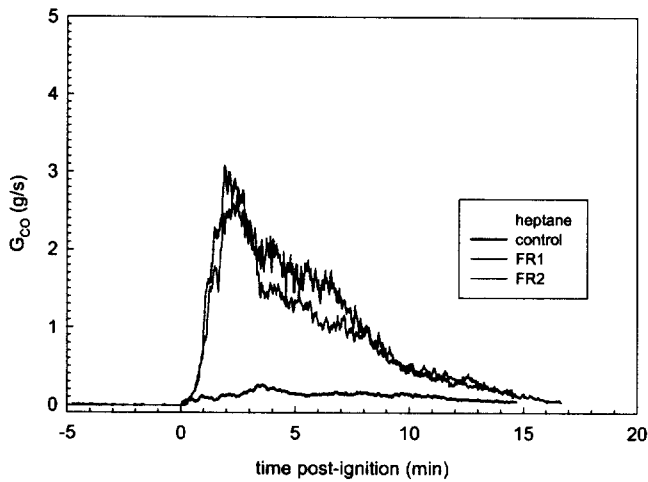


Figure 4. Carbon monoxide release rate (G_{CO}) curves.

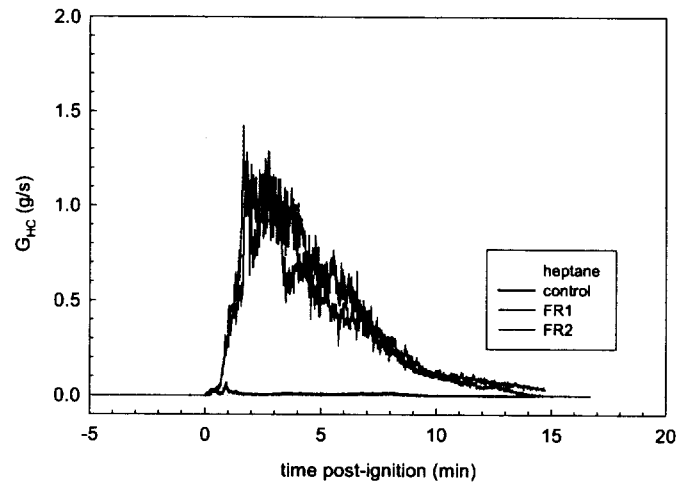


Figure 5. Hydrocarbon release rate (G_{HC}) curves.

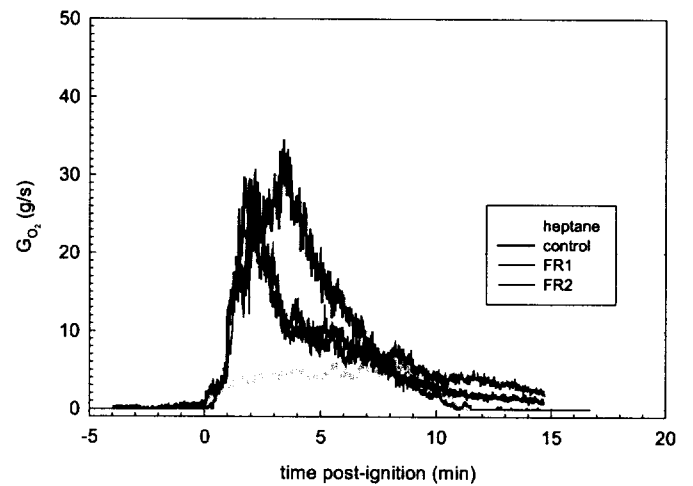


Figure 6. Oxygen consumption rate (G_{O_2}) curves.

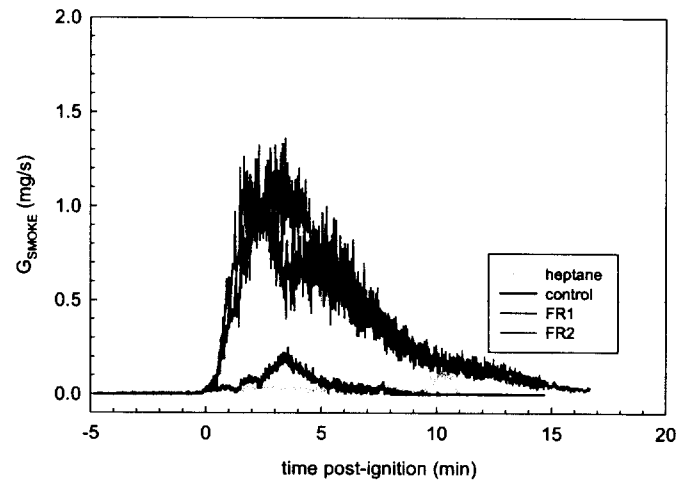


Figure 7. Smoke release rate (G_{SMOKE}) curves.

Plots of the convective heat release rate (Q_{CONV}) for the control HVAC module, the two experimental HVAC modules, and the heptane ignition source are shown in Figure 8. Q_{CONV} was determined from the ambient air temperature and the gas temperature in the fire products collector using equation 4.

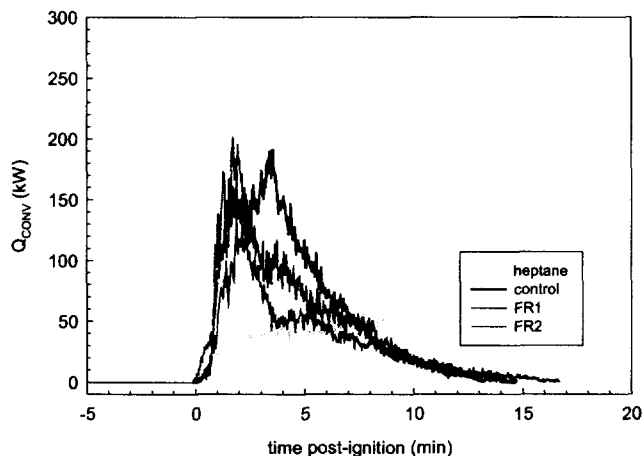


Figure 8. Convective heat release rate (Q_{CONV}) curves.

Plots of the chemical heat release rates for the control HVAC module, the two experimental HVAC modules, and the heptane ignition source are shown in Figures 9 and 10. Figure 9 shows $Q_{CHEM}^{CO_2}$ determined from G_{CO_2} and G_{CO} using equation 5. Figure 10 shows $Q_{CHEM}^{O_2}$ determined from G_{O_2} using equation 6.

The total mass loss, energy yield, carbon dioxide yield, carbon monoxide yield, total hydrocarbon yield, smoke yield, and oxygen consumption for the control HVAC module and the two experimental HVAC modules are shown in Table 3.

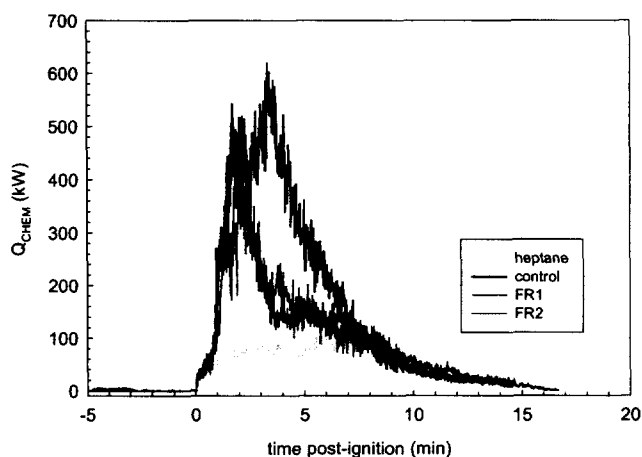


Figure 9. Chemical heat release rate ($Q_{CHEM}^{CO_2}$) curves calculated from G_{CO_2} and G_{CO} .

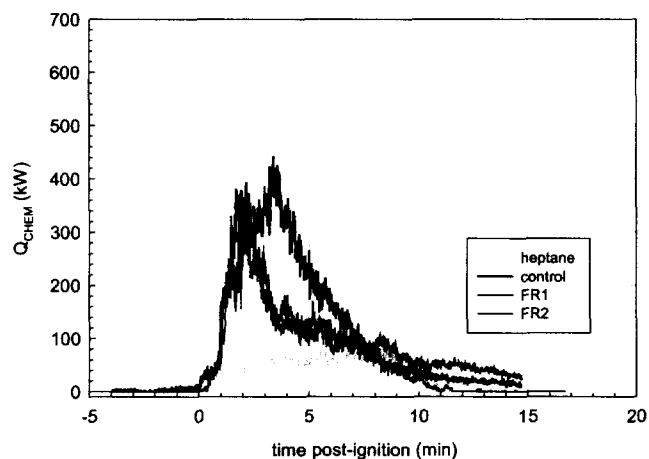


Figure 10. Chemical heat release rate ($Q_{CHEM}^{O_2}$) curves calculated from G_{O_2} .

The mass losses in Table 3 are the final mass losses in Figure 2. The energy yields in Table 3 for the control and experimental HVAC modules were determined by integrating $Q_{CHEM}^{CO_2}$ and $Q_{CHEM}^{O_2}$, and subtracting the values obtained by integrating the curve for the heptane igniter (Fig.'s 9 and 10). The carbon dioxide yield, carbon monoxide yield, total hydrocarbon yield, smoke yield and oxygen consumption were determined by integrating $G_{CO_2} \cdot dt$, $G_{CO} \cdot dt$, $G_{HC} \cdot dt$, $G_{SMOKE} \cdot dt$, and $G_{O_2} \cdot dt$, and subtracting the values obtained by integrating curves for the heptane igniter (Fig.'s 3 through 7).

The energy yields from FR1 and FR2 derived from $Q_{CHEM}^{CO_2}$ were 51 and 46 % of the energy yield from the control. The energy yields from FR1 and FR2 derived from $Q_{CHEM}^{O_2}$ were 42 and 66% of the energy yield from the control. For pure polymers, $Q_{CHEM}^{CO_2}$ is generally considered to be more reliable than $Q_{CHEM}^{O_2}$ because the precision in measuring changes in C_{CO_2} resulting from a fire is greater than the precision in measuring changes in C_{O_2} . The reason for the greater precision in the measurement of C_{CO_2} compared to C_{O_2} is that the concentration of CO_2 in air is between 350 and 400 ppm, while the concentration of O_2 in air is approximately 21% (210,000 ppm). Although the amount (number of molecules) of O_2 consumed when an organic polymer burns is greater than the amount of CO_2 produced, the relative increase in the concentration of CO_2 in air is considerably greater than the relative decrease in the concentration of O_2 . For example, the maximum concentration of CO_2 recorded during the test of the control HVAC module was approximately 1700 ppm, a 480% increase in the CO_2 concentration in air from the background concentration of carbon dioxide (350 to 400

ppm). The minimum concentration of O₂ measured during the test of the control HVAC module was approximately 20.73%, a 1% decrease in the O₂ concentration in ambient air.

Table 3
Summary of Mass Loss, Energy and Chemical Product Yields for the Control and Experimental HVAC Modules

Parameter		CON	FR1	FR2
Mass Loss (g)		4296	4303	4165
Energy Yield (MJ)	$Q_{CHEM}^{CO_2}$	105	54	48
	$Q_{CHEM}^{O_2}$	80	34	53
Carbon Dioxide Yield (g)		7660	3324	2907
Carbon Monoxide Yield (g)		107	960	804
Total Hydrocarbon Yield (g)		6	334	292
Smoke Yield (mg)		8	378	310
Oxygen Consumed (g)		6128	2807	4118

At $t \geq 898^\circ\text{C}$, $\text{Ca}(\text{CO}_3)$ in the form of calcite decomposes to CO_2 and CaO [20]. In cases where $\text{Ca}(\text{CO}_3)$ liberates CO_2 during combustion, $Q_{CHEM}^{CO_2}$ calculated from G_{CO} and G_{CO_2} using equation 5 would be greater than the actual chemical heat release rate of the fire because of the production of CO_2 from a source other than polymer oxidation. Calcium carbonate in the poly(propylene) components of the control HVAC module appears to have had a small effect on the calculated chemical heat release rate of the control HVAC module. The average of the $G_{CHEM}^{CO_2}$ calculated for FR1 and FR2 was 49% of $G_{CHEM}^{CO_2}$ calculated for the control HVAC module. The average of the $G_{CHEM}^{O_2}$ calculated for FR1 and FR2 was 54% of $G_{CHEM}^{O_2}$ calculated for the control HVAC module.

The yield of incomplete oxidation products, which includes carbon monoxide, total hydrocarbons, and smoke, was greater from FR1 and FR2 than from the control HVAC module. The yields of carbon monoxide from FR1 and FR2 were 897 and 751% of the yield of carbon monoxide from the control HVAC module (Table 3). The yields of total hydrocarbon from FR1 and FR2 were 5,567 and 4,867% of the yield of total hydrocarbons from the control HVAC module (Table 3).

The yields of smoke from FR1 and FR2 were 4,725 and 3,875% of the yield of smoke from the control HVAC

module (Table 3), which is consistent with visual observations made during these tests that FR1 and FR2 produced substantially more smoke than the control HVAC module.

Discussion

Decomposition of the polymers and volatilization of the thermal decomposition products yielded qualitatively similar fuels and occurred at similar rates in the control and the two experimental HVAC modules. Chemical analysis of pyrolysate from a poly(propylene) resin without additives and the poly(propylene) resin used in FR1 and FR2 indicated that both resins produced a mixture of methyl-branched saturated and unsaturated aliphatic hydrocarbons [21]. Addition of flame retardants to the poly(propylene) and polyester resins resulted in a shift toward lower molecular weight compounds in the pyrolysate, but did not appear to measurably affect the total quantity of thermal decomposition products from the poly(propylene) [21]. As indicated by the similar mass loss rates (Fig. 2) and total mass losses (Table 3) of the control and two experimental HVAC modules in this study, the use of polymers containing flame retardant additives did not result in measurable differences in the mass loss characteristics of the HVAC modules when exposed to burning heptane.

Flame retardant chemical additives did affect the burning characteristics of the HVAC modules, resulting in less efficient combustion and lower heat release rates. As indicated by oxygen consumption rates, carbon dioxide release rates, and heat release rates, the rates of fuel consumption and heat production were lower in the tests of FR1 and FR2 than in the test of the control HVAC module. Increases in the carbon monoxide release rates, total hydrocarbon release rate, and smoke release rate indicate that oxidization in the combustion zone of the thermal decomposition products from the polymers was less efficient in the tests of FR1 and FR2 than in the test of the control HVAC module.

These results suggest that the principle mechanism of action of the flame retardants used in this study was to inhibit the gas phase chemical reactions consuming oxygen and fuel and producing heat in the combustion zone. This resulted in less efficient combustion with concomitant lower heat release rates and greater production of carbon monoxide, smoke, and other products of incomplete combustion.

References

1. Carlos J. Hilaldo. Flammability Handbook for Plastics. Third Edition. Technomic Publication Co., Westport CT., 1982.

2. Jurgen Troitzsch. International Plastics Flammability Handbook. Principles Regulations Testing and Approval. Second Edition. Hanser Gruber Publishers, Munich, 1991.
3. Fred Shafizadeh, Ping-Sen Chin, and William F. DeGroot. Mechanistic evaluation of flame retardants. *J. Fire Retardant Chem.* 2:195-203, 1975.
4. Richard G. Bauer. Fire retardant Polymers: A review. *J. Fire Retardant Chem.* 5200-221, 1978.
5. Eric R. Larsen. Mechanism of flame inhibition II. A new principle of flame suppression. *J. Fire Retardant Chem.* 2:5-20, 1975.
6. Sharon K. Bauman. Phosphorous fire retardance in polymers. I. General Mode of action. *J. Fire Retardant Chem.* 4:18-37, 1977.
7. Sharon K. Bauman. Phosphorous fire retardance in polymers. II. Retardant-polymer substrate interactions. *J. Fire Retardant Chem.* 4:38-58, 1977.
8. Sharon K. Bauman. Phosphorous fire retardance in polymers. III. Some aspects of combustion performance. *J. Fire Retardant Chem.* 4:93-111 1977.
9. James E. Bostic and Robert H. Barker. Pyrolysis and combustion of polyester. Part II. Effect of triphenylphosphene oxide as a flame retardant. *J. Fire Retardant Chem.* 4:165-182, 1977.
10. William C. McNeill, Michael J. Drews, and Robert H. Barker. Pyrolysis and combustion of polyester. Part III. Brominated fire retardants in poly(ethylene terphthalate). *J. Fire Retardant Chem.* 4:222-234, 1977.
11. Yoichi Uehara and Shosuke Suzuki. The effect of chlorinated polyethylene on the combustion of polyethylene. *J. Fire Retardant Chem.* 6:451-467, 1975.
12. Sharon K. Brauman and Archibald S. Brolly. Sb_2O_3 -halogen fire retardance in polymers I. General mode of action. *J. Fire Retardant Chem.* 3:66-83, 1976.
13. Sharon K. Brauman. Sb_2O_3 -halogen fire retardance in polymers II. Antimony-halogen substrate interactions. *J. Fire Retardant Chem.* 3:117-137, 1976.
14. Sharon K. Brauma. Sb_2O_3 -halogen fire retardance in polymers III. Retardant-polymer substrate interactions. *J. Fire Retardant Chem.* 3:138-163, 1976.
15. Sharon K. Brauman, Norman Fishman, Archibald S. Brolly, and David L. Chamberlain. Sb_2O_3 -halogen fire retardance in polymers IV. Combustion performance. *J. Fire Retardant Chem.* 3:225-264, 1976.
16. Elias A. Woycheshin and Igor Sobolev. Effect of particle size on the performance of alumina hydrate in glass-reinforced polyesters. *J. Fire Retardant Chem.* 2:224-241, 1975.
17. D. A. Purser. "The Development of Toxic Hazard in Fires from Polyurethane Foams and the Effects of Fire Retardants." In *Proceedings of Flame Retardants 90*, British Plastics Federation, Elsevier, London, 1990. pp. 206-221.
18. G. Heskestad. A Fire Products Collector for Calorimetry into the MW Range, Technical Report J.I. OC2E1.RA. Factory Mutual Research Corporation, Norwood, MA. June, 1981.
19. Archibald Tewarson. "Generation of Heat and Chemical Compounds in Fires" in Section 3/Chapter 4, *SFPE Handbook of Fire Protection Engineering*, 2nd Edition, 1995, pp. 3:53-124.
20. Handbook of Chemistry and Physics, 54th Edition, 1973-1974, The Chemical Rubber Company Press, Cleveland, Ohio. p. B-77.
21. Jeffrey Santrock, unpublished data.